Epigenetic therapy to enhance therapeutic effects of PD-1 inhibition in therapy-resistant melanoma

Vasu R. Sah[a], Joakim Karlsson[a,b], Henrik Jespersen[c,d], Mattias F. Lindberg[a], Lisa M. Nilsson[a,b], Lars Ny[c] and Jonas A. Nilsson[a,b,*]

Targeted therapy and immunotherapy have revolutionized the treatment of metastatic skin melanoma but around half of all patients develop resistance early or late during treatment. The situation is even worse for patients with metastatic uveal melanoma (UM). Here we hypothesized that the immunotherapy of therapy-resistant skin melanoma or UM can be enhanced by epigenetic inhibitors. Cultured B16F10 cells and human UM cells were treated with the histone deacetylase inhibitor (HDACi) entinostat or BETi JQ1. Entinostat-induced HLA expression and PD-L1, but JQ1 did not. A syngeneic mouse model carrying B16-F10 melanoma cells was treated with PD-1 and CTLA4 inhibitors, which was curative. Co-treatment with the bioavailable BETi iBET726 impaired the immunotherapy effect. Monotherapy of a B16-F10 mouse model with anti-PD-1 resulted in a moderate therapeutic effect that could be enhanced by entinostat. Mice carrying PD-L1 knockout B16-F10 cells were also sensitive to entinostat. This suggests HDAC inhibition and immunotherapy could work in concert. Indeed, co-cultures of UM with HLA-matched melanoma-specific tumor-infiltrating lymphocytes (TILs) resulted in higher TIL-mediated melanoma killing when entinostat was added. Further exploration of combined immunotherapy and epigenetic therapy in metastatic melanoma resistant to PD-1 inhibition is warranted. *Melanoma Res* 32: 241–248 Copyright © 2021 The Author(s). Published by Wolters Kluwer Health, Inc.

Introduction

Targeted therapies and immune checkpoint inhibitors have revolutionized the treatment of metastatic cutaneous melanoma [1–3], but half of all patients develop or are already resistant to therapy. Resistance mechanisms include low tumor mutational burden (TMB) [4], poor antigen processing and presentation, and immune-suppressive tumor microenvironments (TME) [5–7], as well as a change in differentiation status of the melanoma favoring a more neural-crest like cell that down-regulates immunogenic melanoma-associated antigens and is highly plastic.

One subtype of melanoma that is inherently resistant to immunotherapy is uveal melanoma (UM). It is a rare form of melanoma, with an incidence of approximately eight new cases per million per year in Sweden [8]. UMs originate from choroid, ciliary body or iris melanocytes and are clinically and biologically different from cutaneous melanoma [9,10]. The primary disease can in most cases be successfully treated with radiotherapy or enucleation, but half of the patients subsequently develop metastatic disease, usually to the liver [11,12]. There are still no approved treatments for patients with metastatic UM, who have a median survival of less than 12 months [13].

UM harbors oncogenic mutations in the genes encoding the G-protein-alpha proteins *GNAQ* or the mutually exclusive *GNA11*, *PLCB4* or *CYSLTR2*, and poor prognosis is associated with monosomy of chromosome 3 (Chr. 3) and inactivating mutations of the *BAP1* tumor suppressor gene [14–17]. Therefore, BRAF inhibitors frequently used in skin melanoma do not work in UM. Outcomes with immune checkpoint inhibitor monotherapy have been disappointing, with response rates typically below 5% [18,19]. Despite this, there appears to be some level of immunity against UM, since expanded and adoptively transferred tumor-infiltrating lymphocytes (TILs) have therapeutic clinical effects [17,20]. Tebentafusp, a bispecific protein immunotherapy targeting CD3 and melanoma-specific gp100, has also shown activity in early-phase clinical

studies [21], and combined PD-1 and CTLA4 immune checkpoint inhibition appears to be more effective than monotherapy, albeit not as effective as in cutaneous melanoma [22].

With the notable exception of iris melanomas, which display a UV damage mutational signature [17], most UM display low TMB [4]. Other factors that could mediate poor responses to immunotherapy could be poor antigen processing and presentation or immune-suppressive TMEs [5–7], especially in the liver [23]. Drugs targeting epigenetic regulators such as histone deacetylases (HDACs), BET bromodomain proteins, and methyltransferases are showing promise as cancer therapies by reversing oncogene transcription and modifying the TME [24]. HDAC inhibitors (HDACi) block the effects of myeloid-derived suppressor cells (MDSCs) and regulatory T cells (Tregs) [25,26]; they enhance the expression of cancer antigens silenced during immunoediting [27]; or they trigger DNA damage and cell death to activate danger signals and recruit immune cells [28,29]. Finally, HDACi can increase HLA class I expression, resulting in enhanced antigen presentation [30].

The checkpoint ligand PD-L1 is usually induced when T cells meet cancer cells but HDACi can directly induce PD-L1 to inactivate T cells [31]. This is contrary to BET inhibitors (BETi) in some tumor types where PD-L1 is suppressed [32]. Nuclear acetylated PD-L1 was recently shown to stimulate antigen presentation [33], providing a potential explanation for why PD-L1-high tumors are sensitive to PD-1 inhibition. Since PD-L1 is induced by HDACi this suggests that anti-PD-1 therapies and HDACi could synergize. Previous in-vivo preclinical studies [26,31,34–38] and phase I/II trials have shown encouraging results when combining the HDACi with PD-1 immunotherapy [39–42], most recently in the PEMDAC trial of metastatic UM [43].

Here we report on preclinical examination supporting the use of HDACi and not BETi to increase immunogenicity of therapy-resistant melanoma including UM. We find that HDACi induces HLA molecules, PD-L1, and synergizes with TIL killing *in vitro* and PD-1 immunotherapy in an animal model.

Methods
Cell culture
B16-F10, a murine melanoma cell line, was obtained from Cell Lines Services (Eppelheim, Germany), while 92-1, MEL202 and MP41, three human uveal cell lines, were obtained from the EACC and ATCC, respectively. UM22, a human UM cell line derived from a patient with UM [17], was grown in culture and used for further experiments. All cells were maintained in complete medium (RPMI-1640 supplemented with 10% FBS, glutamine, and gentamycin) and cultured at 37 °C with 5% CO_2. Cell line validation was performed by RNAseq where known

and unique combinations of GNAQ/GNA11/SF3B1/EIF1AX/BAP1 driver mutations were confirmed.

To generate a *Cd274* (PD-L1) CRISPR/Cas9 knockout B16-F10 cell line, Cas9:crRNA:tracrRNA ribonucleoprotein complex was assembled according to the manufacturer's recommendations (Integrated DNA Technologies, Coralville, IA) and transfected into cells using Neon electroporation (Thermo Fisher Scientific, Waltham, Massachusetts, USA). Negative cells were sorted for the absence of PD-L1 by staining with a PE-labeled anti-mouse PD-L1 antibody (clone MIH5; BD Biosciences, Franklin Lakes, New Jersey, USA) using a FACSAria III (BD Biosciences). The absence of PD-L1 expression in the PD-L1 knockout cells was confirmed in cells treated with entinostat (Selleck Chemicals, Houston, Texas, USA) to induce PD-L1.

Generation of MART-1 specific T cells
MART-1-specific T cells from UM biopsies were identified as previously described (13) and sorted using FACSAria III (BD Biosciences). Sorted MART-1-specific T cells were co-cultured with irradiated allogenic peripheral blood leukocytes at a 1:200 ratio in AIM-V cell culture medium (Invitrogen, Carlsbad, California, USA) supplemented with 6000 IU recombinant IL-2 (PeproTech, Rocky Hill, New Jersey, USA), 10% human AB serum (Sigma Aldrich, St Louis, Missouri, USA), and 30 ng/ml CD3 antibody (clone OKT3; Miltenyi Biotech, Bergisch Gladbach, Germany) for 14 days with regular media changes. After completion of the expansion protocol, MART-1 specificity was confirmed using MART-1-specific dextramers (Immudex, Copenhagen, Denmark).

Animal experiments
All animal experiments were performed in accordance with EU Directives (regional animal ethics committee of Gothenburg #2021/19). Tumor models of parental B16-F10-luciferase or PD-L1-knockout B16-F10-luciferase cells were established by injecting 7.5×10^4 cells per mouse mixed with an equal volume of Matrigel (Corning Inc., Corning, New York, USA) subcutaneously into the flanks of 4–6-week-old C57BL6 mice. Tumors were measured with calipers at regular intervals and tumor volumes calculated using the formula: tumor volume (mm^3) = [length (mm)] × [width (mm) × width (mm)]/2. Three days after transplantation, sedated mice were injected with 100 µl (30 mg/ml D-luciferin) in an isoflurane administrating chamber and then placed in an IVIS Lumina III XR machine (Perkin Elmer, Norwalk, Connecticut, USA). IVIS values on day three post tumor implantation were taken to allocate mice into balanced treatment groups of PBS-injected, 200 µg PD-1-blocking antibody-injected (clone RMP1-14; BioXCell, Lebanon, New Hampshire, USA) intraperitoneally twice per week for three weeks, entinostat-treated (food containing 50 mg/kg entinostat), or a combination of PD-1-blocking antibody-injected

and entinostat-treated mice. For iBET immunotherapy combination, mice were treated with vehicle or iBET726 orally (10 mg/kg) once daily for seven days, 250 µg PD-1 and CTLA4 blocking (clone 9H10; BioXCell) antibodies were injected intraperitoneally thrice per week for 4 weeks or a combination of PD-1 and CTLA4 antibodies with iBET762 were used.

Cell staining and in-vitro assays

Tumor cells were seeded and treated with entinostat (1 µM) or JQ1 (1 µM) for 48 hours and thereafter stained for 30 minutes at 4 °C with specific antibodies for flow cytometry. The following anti-human antibodies were used for surface staining: FITC-labeled mouse anti-human HLA-DR, -DP, -DQ (Clone Tu39; BD Biosciences); PE-labeled mouse anti-human HLA-ABC (Clone G46-2.6; BD Biosciences); and APC-labeled mouse anti-human PD-L1 (clone 29E2A3; Biolegend, San Diego, California, USA). The following anti-mouse antibodies we used for surface staining: Alexa Fluor 647-labeled H-2Kb/H-2Db - MHC Class I (clone 28-8-6, Biolegend); PE-labeled I-A/I-E – MHC Class II (Clone M5/114.15.2; BD Biosciences), and PE-labeled PD-L1 (clone MIH5; BD Biosciences). Dead cells were excluded from the analysis by applying gating strategies.

Tumor cells were seeded in 24-well plates and treated with entinostat (1 µM), MART-1+ REP TILs in a 1:5 ratio with tumor cells, and 30 µg/ml pembrolizumab. 48 hours later, all cells were fixed and permeabilized using the Fixation/Permeabilization Solution Kit (554714, BD Biosciences) and then incubated with FITC-labeled rabbit anti-active caspase-3 (clone C92-605; BD Biosciences) and PE-labeled mouse anti-human granzyme B (clone GB11; BD Biosciences) antibodies for 30 minutes at 4 °C. Flow cytometry data were acquired using BD Accuri C6 and BD Accuri C6 plus (BD Biosciences).

Tumor-bearing mice were sacrificed and single-cell suspensions were generated from tumors and spleens using mechanical dissociation before being passed through a 70 µm filter. Tumor suspensions were stained with 7-AAD live/dead stain (Miltenyi Biotec, Woking, UK), FITC-labeled CD3e (clone-145-2C11; BD Biosciences), PE-labeled CD4 (clone GK1.5; Biolegend), and APC-labeled CD8a (clone 53-6.7; BD Biosciences) for analysis of TILs. A seven-color myeloid panel with BUV395-labeled CD45 (clone 30-F11, BD Biosciences), Alexa Fluor 700-labeled F4/80 (clone BM8; BD Biosciences), brilliant violet 421-labeled Ly-6G (clone 1A8; Biolegend), PE/cyanine7-labeled Ly-6C (clone HK1.4; Biolegend), brilliant violet 605-labeled CD206 (MMR) (clone C068C2; Biolegend), BUV737-labeled CD11b (clone M1/70; BD Biosciences), and live/dead yellow stain (Thermo Fisher Scientific) was created for analysis of tumor samples. The proportions of tumor-infiltrating myeloid cells (CD45+CD11b+),

monocytic MDSCs (CD45+CD11b+Ly6c+), "M2-like" TAMs (CD45+CD11b+CD206+), non "M2-like" TAMs (CD45+CD11b+CD206-), and Mo-MDSC +M2-like TAMs+ (CD45+CD11b+Ly6c+CD206+) were acquired on a BD LSRII flow cytometer using FACSDiva software (BD Biosciences) for acquisition and compensation and then analyzed using FlowJo software.

Statistical analysis

For flow cytometry measurements of HLA genes and PD-L1 in 92-1, MEL202, and MP41 cells, and independently for H-2Kb/H-2Db and I-A/I-E, unpaired two-tailed t-tests were carried out to assess effects of treatment with entinostat with the t.test function in R (v. 3.6.0, default parameters). Normality was assessed with Shapiro−Wilk tests, using the shapiro.test function in R. For differences in cell-type proportions estimated by flow cytometry, as well as regarding proportions of cells with cleaved caspase-3 or granzyme B, unpaired two-sample *t*-tests were used. For analysis of tumor growth in in-vivo experiments, the compareGrowthCurves function in the statmod R package (v. 1.4.32) with the parameter nsim = 10^5 was used. For survival analysis of in-vivo experiments, log-rank tests were performed with the survdiff function from the survival R package (v. 3.2-7) with the parameter rho = 0. *P*-values were adjusted for multiple testing with the Benjamini-Hochberg method. All statistical tests in this study were two-sided, and all error bars represent SEM, unless otherwise stated. A complete set of statistical tests in the study are present in Supplementary Table 1, Supplemental digital content 1, *http://links.lww.com/MR/A282*.

Results
Entinostat alters the transcriptome of immune-related genes in uveal melanoma cells

To assess the effect of HDAC inhibition on HLA and PD-L1 expression, the human UM cell lines 92-1 (mutations in GNAQ and EIF1AX, derived from a primary eye tumor), MEL202 (mutant GNAQ and SF3B1, primary tumor), MP41 (mutant GNA11, monosomy Chr. 3, primary tumor) and UM22 (mutant GNAQ and BAP1, metastasis) were treated with the HDACi entinostat and analyzed by flow cytometry. Entinostat-induced HLA-ABC in 92-1, MEL202, and UM22 UM cells, but HLA-ABC was already highly expressed in MP41 cells and not further induced (Fig. 1a, gating strategy shown in Supplementary Fig. 1, Supplemental digital content 2, *http://links.lww.com/MR/A276*). PD-L1 was induced by entinostat in all cell lines (Fig. 1b). To gain further insight into immune-related expression changes, gene expression changes following entinostat treatment were analyzed by RNA sequencing. This analysis confirmed induction of HLA genes or CD274 (PD-L1) with RNAseq for UM22, MP41, and 92-1 (Fig. 1c and Supplementary Table 2, Supplemental digital content 3, *http://links.lww.com/MR/A281*). Entinostat

Fig. 1
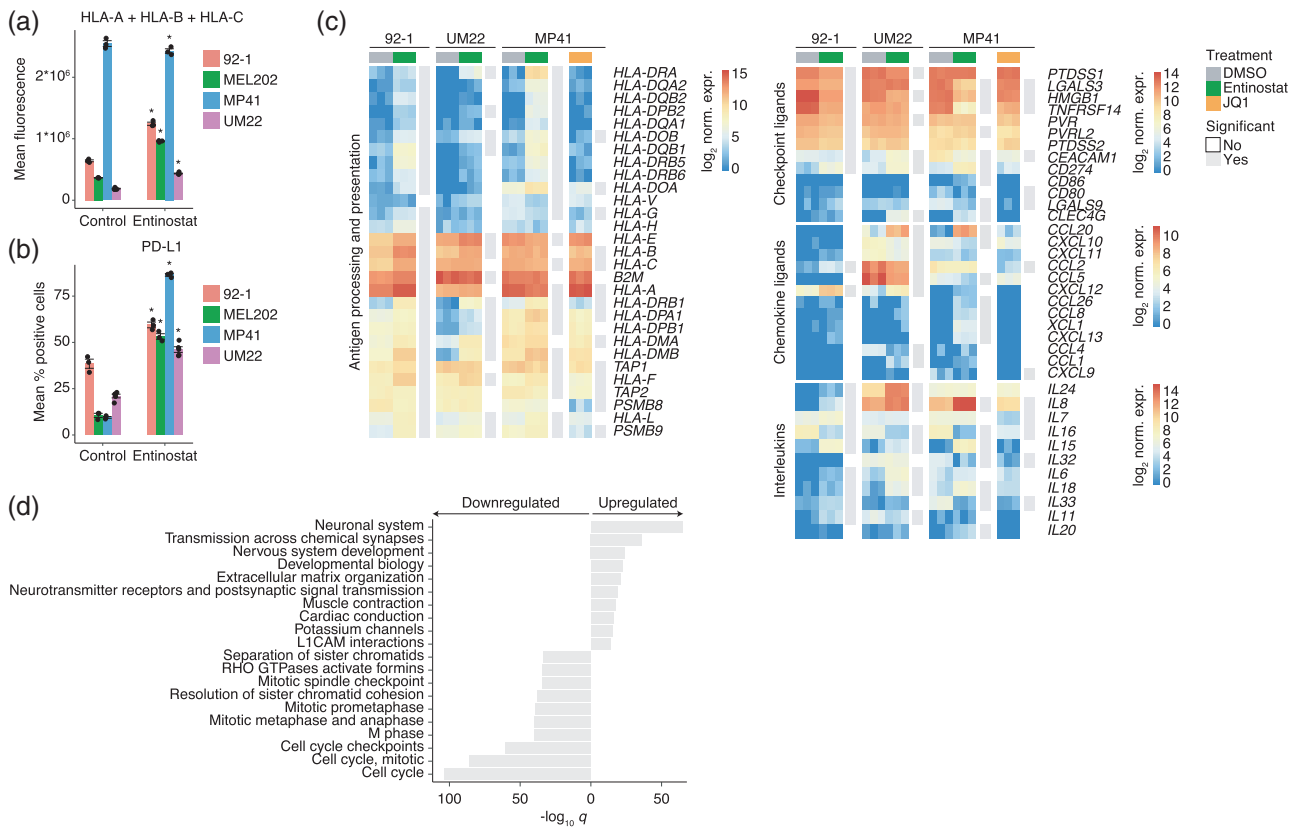
Entinostat regulates the expression of immune-associated genes in human UM cell lines. (a and b) Human UM cell lines 92-1, MEL202, MP41 and UM22 have been treated with DMSO or 1 μM entinostat for 48 hours. Flow cytometry of (a) human HLA-ABC expression (mean fluorescence intensity) and (b) human PD-L1 expression (% positive cells compared to unstained control). $n = 3$ biological replicates per cell line and condition were used, except for UM22, where $n = 5$ and $n = 1$ replicates were used. Significance was assessed with t-tests and adjusted P-values <0.05 were considered statistically significant, as indicated with asterisks. (c) Differentially expressed immune-associated genes in the human UM cell lines 92-1, MP41 and UM22 after treatment with entinostat for 48 hours compared to DMSO ($n = 3$ biological replicates per condition). Genes with FDR-adjusted P-values <0.05 were considered statistically significant. Statistical tests were carried out using DESeq2. Asterisks indicate genes significant in all three cell lines, whereas individual cell line-specific significance is indicated in gray next to each heatmap. (d) Enriched Reactome pathways among genes with adjusted P-values <0.05 and absolute log$_2$ fold change >2 in all three cell lines, assessed with the MSigDB gene set enrichment analysis tool.

also induced the immune proteasome gene PSMB9 and T cell cytokine genes IL15 and CXCL12 but not the ABC transporters TAP1 and TAP2. Expression of the immune checkpoint protein TIM3 ligand HMGB1 was suppressed in all cell lines and the ligand CEACAM1 in all except UM22 (Fig. 1c and Supplementary Fig. 2a,b, Supplemental digital content 2, *http://links.lww.com/MR/A276*). These effects were not seen with the BET bromo-domain inhibitor (BETi) JQ1 (Fig. 1c).

Entinostat increases the anti-tumoral effects of T cells *in vivo* and *in vitro*

To assess the immune-modulatory effect of HDACi and BETi in an immune-competent and syngeneic mouse transplant model we used the B16-F10 murine melanoma cells. Although these tumors did not originate from the uvea of the eye, B16-F10 cells resemble UM in that they

are immunotherapy-resistant, do not harbor classical cutaneous melanoma BRAF, NRAS, or NF1 mutations and the TMB is low [44]. Entinostat-induced surface expression of MHC class I and II and PD-L1 (Fig. 2a and Supplementary Table 1, Supplemental digital content 1, *http://links.lww.com/MR/A282*), similar to in human UM cells.

Next, we tested the in-vivo efficacy of combined HDAC and PD-1 inhibition in C57/BL6 mice transplanted with subcutaneous B16-F10 tumors. Treatment with entinostat resulted in faster tumor growth than vehicle controls and PD-1 inhibitor alone did not inhibit tumor growth (Fig. 2b and c). However, combined entinostat and PD-1 inhibitor significantly delayed tumor growth and prolonged survival compared to monotherapy (Fig. 2b and c). Combination treatment also increased intra-tumoral CD8$^+$ T cells (but not CD4$^+$ cells) and decreased both tumor-infiltrating myeloid cells and monocytic MDSCs.

Fig. 2
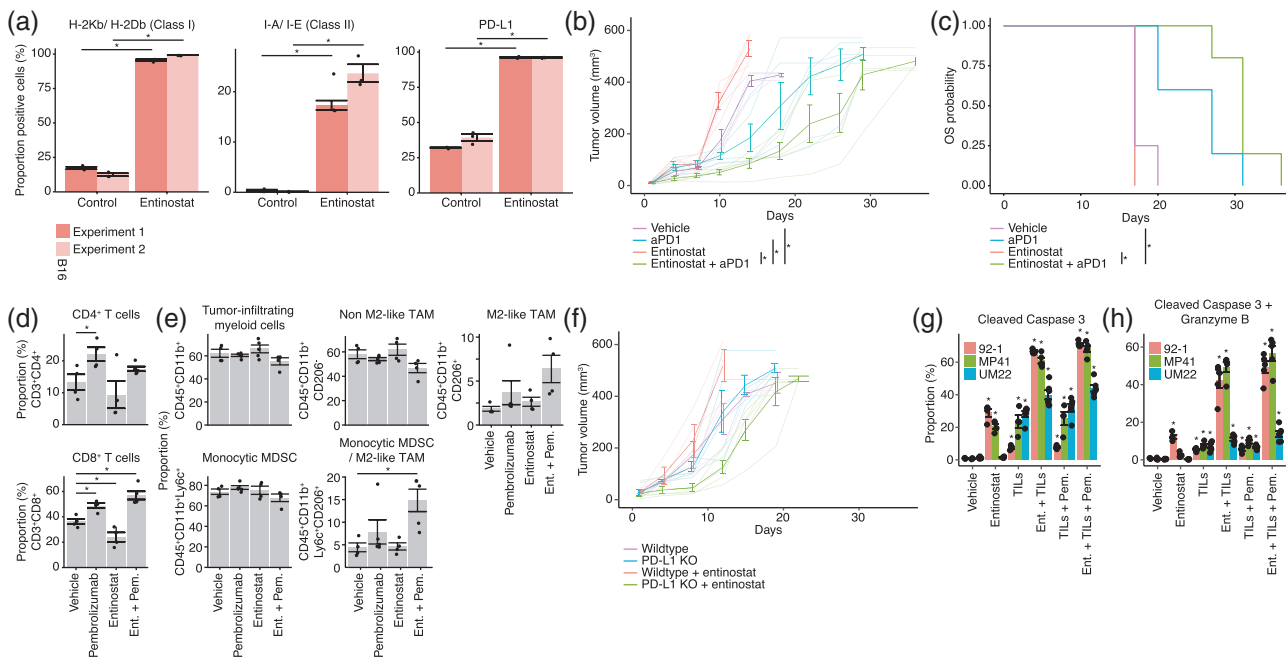
Entinostat enhances immunotherapy *in vitro* and *in vivo*. (a) Flow cytometry analysis showing HLA class 1, class 2 and PD-L1 expression in B16-F10 melanoma cells treated with entinostat. The experiment was repeated twice with *n* = 3 biological replicates each time. Asterisks indicate significance between vehicle and control. (b and c) Eighteen C57BL6 mice with subcutaneous B16-F10-luciferase tumors were allocated to groups to receive treatment with vehicle (*n* = 4), entinostat (*n* = 4), PD-1 inhibitor (aPD1, *n* = 5), or the combination of entinostat and PD-1 inhibitor (*n* = 5). Tumors were measured with calipers and are plotted as mean volumes (bold lines) and individual volumes (light-colored lines) (b). Asterisks indicate *P* < 0.05 as assessed with the 'compareGrowthCurves' function in the statmod R package. Survival was plotted as a Kaplan–Meier curve (c). (d and e) End-of-study tumors samples from mice treated with indicated treatments were analyzed by flow cytometry to assess the distribution of tumor-infiltrating lymphocytes (d) and myeloid cells (e). For (d), *n* = 4 biological replicates were used per condition, except for the combination treatment, where *n* = 5 replicates were used. For (e), *n* = 4 biological replicates were used per condition, except for all treatments with PD1 inhibitor, treatments with entinostat in the experiment measuring CD45+CD11b+ cells, and treatment with entinostat + PD1 inhibitor in the experiment measuring CD45+CD11b+Ly6c+CD206+ cells, where *n* = 5 replicates were used. (f) Sixteen C57BL6 mice were injected subcutaneously with B16-F10-luciferase cells (*n* = 6) or PD-L1-deficient CRISPR B16-F10-luciferase cells (*n* = 10). Half of the animals in both groups received food containing entinostat. Tumors were measured with calipers and are plotted as mean volume (bold lines) and individual volumes (light-colored lines). (g and h) HLA-A2:01-positive human UM cell lines 92-1, MP41 and UM22 were treated with DMSO, 1 μM entinostat, and 30 μg/ml pembrolizumab for 48 hours with or without MART-1-specific T cells for the last 24 hours. Cells were fixed, permeabilized, and stained with antibodies targeting cleaved caspase-3 and granzyme B followed by flow cytometric analysis. Shown are the proportions of double-positive and single-positive melanoma cells. *n* = 4 biological replicates used per cell line and condition, except for assays with the combinations entinostat + TILs and entinostat + pembrolizumab + TILs, where *n* = 5 replicates were used. Significance of differences relative to vehicle (DMSO) were assessed with the two-tailed *t*-test and adjusted (Benjamini-Hochberg correction) *P*-values <0.05 are indicated with an asterisk.

There was also a shift in macrophage phenotype, with increased proportions of pro-tumorigenic "M2-like" tumor-associated macrophages (TAMs) in combination therapy tumors (Fig. 2d and e).

CRISPR/Cas9 inactivation of *Cd274* (PD-L1) in implanted B16-F10 cells (Supplementary Fig. S2c, Supplemental digital content 2, *http://links.lww.com/MR/A276*) did not result in a slower tumor growth but it did improve the faster growth induced by entinostat in parental B16-F10 cells. In fact, *Cd274* knockout cells grew slower than parental cells when treated with entinostat, consistent with the results from the pharmacological combination treatment (Fig. 2f). To investigate whether entinostat could impact on T cell killing of human UM cells, MART-1-specific T cells were isolated from an UM tumor using HLA-A2-specific MART-1 tetramers,

expanded, and then used in killing assays. Incubation of HLA-A2-positive 92-1 and MP41 cells with MART-1-specific T cells induced UM cell apoptosis as measured by cleavage of caspase-3 and deposition of granzyme B (Fig. 2g and h). The addition of anti-PD-1 pembrolizumab only moderately increased T cell killing.

Collectively, these data suggest that combined immune checkpoint blockade and HDAC inhibition can stimulate T cell immunity against human UM *in vitro* and BRAF, NRAS, and NF1 wildtype melanoma *in vivo*.

BET inhibition does not improve immunotherapy *in vivo*
The finding that BETi JQ1 did not induce similar transcriptional changes as did entinostat (Fig. 1c) prompted further investigation into if BET inhibition would impact immunotherapy. Flow cytometry analysis of BETi-treated

Fig. 3
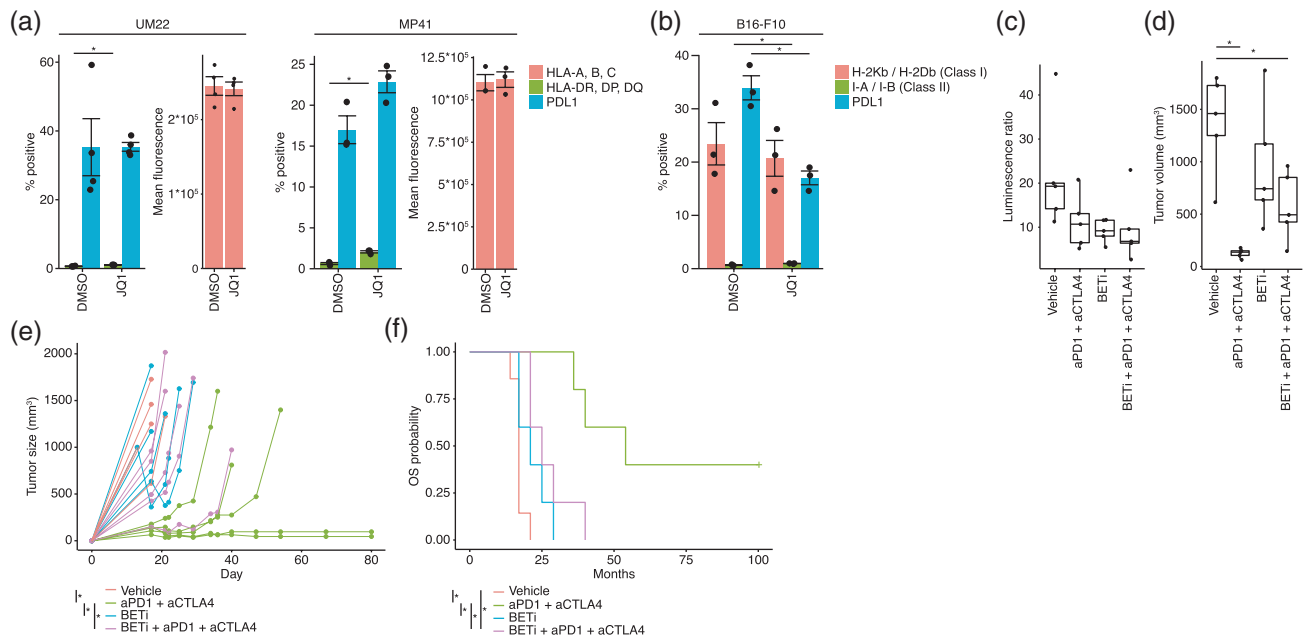
BET inhibition inhibits the expression of MHC class 1 and PD-L1 and the effect of immune checkpoint inhibition *in vivo*. (a) Flow cytometry of MHC class 1, MHC Class 2 and PD-L1 expression, in the uveal melanoma cell lines UM22 and MP41 treated with the vehicle DMSO or 1 μM of the BET inhibitor JQ1 for 48 hours. (b) Flow cytometry of MHC class 1 expression and PD-L1 expression in the mouse melanoma cell line B16-F10 treated with the vehicle DMSO or 1 μM of the BET inhibitor JQ1 for 48 hours. The experiments were repeated twice with $n = 3$ biological replicates for B16-F10, MP41 and for UM22, $n = 4$ and $n = 2$ replicates were analyzed. Asterisks indicate $P < 0.05$ with two-tailed t-tests. (c–f) Twenty C57BL6 mice with subcutaneous B16-F10-luciferase tumors were allocated in groups to receive treatment with vehicle ($n = 5$), CTLA4 + PD1 inhibitors ($n = 5$), iBET762 or combined iBET762 and CTLA4 + PD1 inhibitor. One week after treatment initiation, mice were imaged and luciferase activity was plotted (c). Tumors were also measured 3 weeks after treatment initiation (d) and followed until reaching the ethics limit or up to 80 days post-transplantation (e). In (e), asterisks indicate $P < 0.05$ with two-tailed t-tests. Survival was plotted as the time until the mice reached the ethics limit and were sacrificed (f). In (e) and (f) asterisks indicate adjusted P-values <0.05, as assessed with the compareGrowth-Curves function of the statmod R package in (e) and log-rank tests in (f).

cells confirmed the RNAseq data and showed that HLA class 1 and 2 and PD-L1 expression was unchanged in UM22 cells and MP41 following treatment with JQ1 (Fig. 3a). In B16-F10 cells HLA class 1 was unchanged and PD-L1 was suppressed following JQ1 treatment (Fig. 3b), contrary to the effects of entinostat. To assess the impact of BET inhibition *in vivo* we treated B16-F10 melanoma bearing mice with anti-CTLA4 and anti-PD1 antibodies, to ensure better immunotherapy effects than by PD1 inhibition. Concomitant treatment with the bio-available compound iBET726 resulted in a robust early response to treatment (Fig. 3c and d). Long-term the tumors grew back resulting in a worse survival of mice treated with combination BET inhibition and immuno-therapy compared to immunotherapy alone (Fig. 3e and f). This suggests that although BET inhibition can work in monotherapy, it does not improve immunotherapy with PD1/CTLA4 inhibitors.

Discussion

Here we tested the hypothesis that epigenetic modulation can impact immunotherapy. Previous studies have shown that HDACi modulate immune gene expression in cancer, including in HLA genes [30,45]. However, as shown

in other cancer types, and here in mouse melanoma *in vivo* and human UM *in vitro*, the trade-off is that entinostat monotherapy also induced PD-L1 in cancer cells. This may counteract any beneficial immunotherapeutic effects of HDAC inhibition. Indeed, entinostat-treated B16-F10 melanoma cells grew faster, an effect reversed on *Cd274* (PD-L1 gene) knockdown using CRISPR. This provided a strong rationale to combine HDAC and PD-1 inhibition to leverage the positive immune-stimulatory effects of both drugs. However, entinostat-induced PD-L1 expression may play less role for ACT as visualized in our human in vitro experiments, since IL-2 can override the PD-1/PD-L1 axis IL-2 [46]. Moreover, in a system where only T cells and tumor cells are present, and no antigen-presenting cells expressing co-stimulatory molecules, PD-1 inhibitors do not work as immunotherapy [41,42].

BETi have been deemed promising agents for treatment of cancer but a decade after the disclosure of JQ1, no drug has reached a phase III clinical trial. Their mechanism of action is clearly defined in vitro but problems with dose-limiting toxicities, efficacy and resistance have made progress slow thus far in patients. Some of these issues may also be due to the selection of indication as well, since

BETi in parallel to development as anti-cancer drugs also show promise as anti-inflammatory drugs [47]. It may well be that the anti-tumoral effects of BETi are overridden by an inhibition of anti-tumoral immunity. Without powerful elimination of the BET-inhibited cancer cells by immune cells, treatment resistance may form. In the B16-F10 model used herein, we observed that combined anti-PD1 and anti-CTLA4 treatment could result in durable responses in half of the treated mice but if they were also treated with BETi they quickly relapsed. This is in line with previous studies suggesting that BETi can inhibit priming by dendritic cells [48–50] as well as the proliferation [51] or function [52] of T cells. Also NK cell killing is suppressed by BETi via downregulation of NK cell ligands [53]. More experiments are needed to evaluate if there are any conditions where BETi can improve immunotherapy.

The above-described data, and other published data showing that HDAC inhibition stimulates immunotherapy, motivated us to initiate a clinical trial to test combined entinostat and pembrolizumab in patients with metastatic UM (NCT02697630, [54]). In this trial, a correlation between response and survival could be found with the mutational status of the tumor suppressor gene BAP1 [43]. Patients with wildtype BAP1 or one with an iris tumor exhibiting UV damage [17] had a response or longer survival. It is interesting to note that the UM cell lines used here in the preclinical study were three BAP1 wt and one BAP1 mutant cell lines. Since entinostat enhanced TIL killing also of the BAP1 mutant cell line UM22, it may reflect that the BAP1 status may not impact on a tumor-intrinsic property but on an effect of the TME. Indeed, a landmark study by the Coupland laboratory has suggested that BAP1 mutations correlate with an immune suppressive TME [55]. It is therefore plausible that the resistance to immunotherapy in UM is due both to that of TME as well as a low TMB and antigen expression. More studies are needed to disentangle the complex role of loss of BAP1 in UM metastasis and treatment resistance.

Acknowledgements

Data availability: The datasets presented are available at ArrayExpress using accession number E-MTAB-11058.

Conflicts of interest

References

1 Robert C, Long GV, Brady B, Dutriaux C, Maio M, Mortier L, *et al.* Nivolumab in previously untreated melanoma without BRAF mutation. *N Engl J Med* 2015; **372**:320–330.

2 Robert C, Schachter J, Long GV, Arance A, Grob JJ, Mortier L, *et al.*; KEYNOTE-006 investigators. Pembrolizumab versus Ipilimumab in advanced melanoma. *N Engl J Med* 2015; **372**:2521–2532.

3 Larkin J, Chiarion-Sileni V, Gonzalez R, Grob JJ, Rutkowski P, Lao CD, *et al.* Five-year survival with combined nivolumab and ipilimumab in advanced melanoma. *N Engl J Med* 2019; **381**:1535–1546.

4 Royer-Bertrand B, Torsello M, Rimoldi D, El Zaoui I, Cisarova K, Pescini-Gobert R, *et al.* Comprehensive genetic landscape of uveal melanoma by whole-genome sequencing. *Am J Hum Genet* 2016; **99**:1190–1198.

5 Whelchel JC, Farah SE, McLean IW, Burnier MN. Immunohistochemistry of infiltrating lymphocytes in uveal malignant melanoma. *Invest Ophthalmol Vis Sci* 1993; **34**:2603–2606.

6 Maat W, Ly LV, Jordanova ES, de Wolff-Rouendaal D, Schalij-Delfos NE, Jager MJ. Monosomy of chromosome 3 and an inflammatory phenotype occur together in uveal melanoma. *Invest Ophthalmol Vis Sci* 2008; **49**:505–510.

7 Mäkitie T, Summanen P, Tarkkanen A, Kivelä T. Tumor-infiltrating macrophages (CD68(+) cells) and prognosis in malignant uveal melanoma. *Invest Ophthalmol Vis Sci* 2001; **42**:1414–1421.

8 Bergman L, Seregard S, Nilsson B, Ringborg U, Lundell G, Ragnarsson-Olding B. Incidence of uveal melanoma in Sweden from 1960 to 1998. *Invest Ophthalmol Vis Sci* 2002; **43**:2579–2583.

9 Damato B. Treatment of primary intraocular melanoma. *Expert Rev Anticancer Ther* 2006; **6**:493–506.

10 Jager MJ, Shields CL, Cebulla CM, Abdel-Rahman MH, Grossniklaus HE, Stern MH, *et al.* Uveal melanoma. *Nat Rev Dis Primers* 2020; **6**:24.

11 Kujala E, Mäkitie T, Kivelä T. Very long-term prognosis of patients with malignant uveal melanoma. *Invest Ophthalmol Vis Sci* 2003; **44**:4651–4659.

12 Diener-West M, Reynolds SM, Agugliaro DJ, Caldwell R, Cumming K, Earle JD, *et al.*; Collaborative Ocular Melanoma Study Group. Development of metastatic disease after enrollment in the COMS trials for treatment of choroidal melanoma: Collaborative Ocular Melanoma Study Group Report No. 26. *Arch Ophthalmol* 2005; **123**:1639–1643.

13 Khoja L, Atenafu EG, Suciu S, Leyvraz S, Sato T, Marshall E, *et al.* Meta-analysis in metastatic uveal melanoma to determine progression free and overall survival benchmarks: an international rare cancers initiative (IRCI) ocular melanoma study. *Ann Oncol* 2019; **30**:1370–1380.

14 Van Raamsdonk CD, Bezrookove V, Green G, Bauer J, Gaugler L, O'Brien JM, *et al.* Frequent somatic mutations of GNAQ in uveal melanoma and blue naevi. *Nature* 2009; **457**:599–602.

15 Van Raamsdonk CD, Griewank KG, Crosby MB, Garrido MC, Vemula S, Wiesner T, *et al.* Mutations in GNA11 in uveal melanoma. *N Engl J Med* 2010; **363**:2191–2199.

16 Robertson AG, Shih J, Yau C, Gibb EA, Oba J, Mungall KL, *et al.*; TCGA Research Network. Integrative analysis identifies four molecular and clinical subsets in uveal melanoma. *Cancer Cell* 2017; **32**:204–220.e15.

17 Karlsson J, Nilsson LM, Mitra S, Alsén S, Shelke GV, Sah VR, *et al.* Molecular profiling of driver events in metastatic uveal melanoma. *Nat Commun* 2020; **11**:1894.

18 Algazi AP, Tsai KK, Shoushtari AN, Munhoz RR, Eroglu Z, Piulats JM, *et al.* Clinical outcomes in metastatic uveal melanoma treated with PD-1 and PD-L1 antibodies. *Cancer* 2016; **122**:3344–3353.

19 Mignard C, Deschamps Huvier A, Gillibert A, Duval Modeste AB, Dutriaux C, Khammari A, *et al.* Efficacy of immunotherapy in patients with metastatic mucosal or uveal melanoma. *J Oncol* 2018; **2018**:1908065.

20 Chandran SS, Somerville RPT, Yang JC, Sherry RM, Klebanoff CA, Goff SL, *et al.* Treatment of metastatic uveal melanoma with adoptive transfer of tumour-infiltrating lymphocytes: a single-centre, two-stage, single-arm, phase 2 study. *Lancet Oncol* 2017; **18**:792–802.

21 Middleton MR, McAlpine C, Woodcock VK, Corrie P, Infante JR, Steven NM, *et al.* Tebentafusp, A TCR/Anti-CD3 bispecific fusion protein targeting

gp100, potently activated antitumor immune responses in patients with metastatic melanoma. *Clin Cancer Res* 2020; **26**:5869–5878.

22 Pelster MS, Gruschkus SK, Bassett R, Gombos DS, Shephard M, Posada L, *et al.* Nivolumab and Ipilimumab in metastatic uveal melanoma: results from a single-arm phase II study. *J Clin Oncol* 2021; **39**:599–607.

23 Yu J, Green MD, Li S, Sun Y, Journey SN, Choi JE, *et al.* Liver metastasis restrains immunotherapy efficacy via macrophage-mediated T cell elimination. *Nat Med* 2021; **27**:152–164.

24 Topper MJ, Vaz M, Marrone KA, Brahmer JR, Baylin SB. The emerging role of epigenetic therapeutics in immuno-oncology. *Nat Rev Clin Oncol* 2020; **17**:75–90.

25 Shen L, Pili R. Class I histone deacetylase inhibition is a novel mechanism to target regulatory T cells in immunotherapy. *Oncoimmunology* 2012; **1**:948–950.

26 Kim K, Skora AD, Li Z, Liu Q, Tam AJ, Blosser RL, *et al.* Eradication of metastatic mouse cancers resistant to immune checkpoint blockade by suppression of myeloid-derived cells. *Proc Natl Acad Sci U S A* 2014; **111**:11774–11779.

27 Maio M, Coral S, Fratta E, Altomonte M, Sigalotti L. Epigenetic targets for immune intervention in human malignancies. *Oncogene* 2003; **22**:6484–6488.

28 Landreville S, Agapova OA, Matatall KA, Kneass ZT, Onken MD, Lee RS, *et al.* Histone deacetylase inhibitors induce growth arrest and differentiation in uveal melanoma. *Clin Cancer Res* 2012; **18**:408–416.

29 Lee JH, Choy ML, Ngo L, Foster SS, Marks PA. Histone deacetylase inhibitor induces DNA damage, which normal but not transformed cells can repair. *Proc Natl Acad Sci U S A* 2010; **107**:14639–14644.

30 Campoli M, Ferrone S. HLA antigen changes in malignant cells: epigenetic mechanisms and biologic significance. *Oncogene* 2008; **27**:5869–5885.

31 Woods DM, Sodré AL, Villagra A, Sarnaik A, Sotomayor EM, Weber J. HDAC inhibition upregulates PD-1 ligands in melanoma and augments immunotherapy with PD-1 blockade. *Cancer Immunol Res* 2015; **3**:1375–1385.

32 Zhu H, Bengsch F, Svoronos N, Rutkowski MR, Bitler BG, Allegrezza MJ, *et al.* BET bromodomain inhibition promotes anti-tumor immunity by suppressing PD-L1 expression. *Cell Rep* 2016; **16**:2829–2837.

33 Gao Y, Nihira NT, Bu X, Chu C, Zhang J, Kolodziejczyk A, *et al.* Acetylation-dependent regulation of PD-L1 nuclear translocation dictates the efficacy of anti-PD1 immunotherapy. *Nat Cell Biol* 2020; **22**:1064–1075.

34 Zheng H, Zhao W, Yan C, Watson CC, Massengill M, Xie M, *et al.* HDAC inhibitors enhance T-Cell chemokine expression and augment response to PD-1 immunotherapy in lung adenocarcinoma. *Clin Cancer Res* 2016; **22**:4119–4132.

35 Kim YD, Park SM, Ha HC, Lee AR, Won H, Cha H, *et al.* HDAC inhibitor, CG-745, enhances the anti-cancer effect of anti-PD-1 immune checkpoint inhibitor by modulation of the immune microenvironment. *J Cancer* 2020; **11**:4059–4072.

36 Christmas BJ, Rafie CI, Hopkins AC, Scott BA, Ma HS, Cruz KA, *et al.* Entinostat converts immune-resistant breast and pancreatic cancers into checkpoint-responsive tumors by reprogramming tumor-infiltrating MDSCs. *Cancer Immunol Res* 2018; **6**:1561–1577.

37 Orillion A, Hashimoto A, Damayanti N, Shen L, Adelaiye-Ogala R, Arisa S, *et al.* Entinostat neutralizes myeloid-derived suppressor cells and enhances the antitumor effect of PD-1 inhibition in murine models of lung and renal cell carcinoma. *Clin Cancer Res* 2017; **23**:5187–5201.

38 Zimmer L, Livingstone E, Hassel JC, Fluck M, Eigentler T, Loquai C, *et al.*; Dermatologic Cooperative Oncology Group. Adjuvant nivolumab plus ipilimumab or nivolumab monotherapy versus placebo in patients with resected stage IV melanoma with no evidence of disease (IMMUNED): a randomised, double-blind, placebo-controlled, phase 2 trial. *Lancet* 2020; **395**:1558–1568.

39 Sullivan RJ, Moschos SJ, Johnson ML, Opyrchal M, Ordentlich P, Brouwer S, *et al.* Abstract CT072: efficacy and safety of entinostat (ENT) and pembrolizumab (PEMBRO) in patients with melanoma previously treated with anti-PD1 therapy. *Cancer Res* 2019; **79**(13 Suppl):CT072.

40 Gandhi L, Janne PA, Opyrchal M, Ramalingam SS, Rybkin II, Hafez N, *et al.* Efficacy and safety of entinostat (ENT) and pembrolizumab (PEMBRO) in patients with non-small cell lung cancer (NSCLC) previously treated with anti-PD-(L)1 therapy. *J Clin Oncol* 2018; **36**:9036.

41 Hui E, Cheung J, Zhu J, Su X, Taylor MJ, Wallweber HA, *et al.* T cell costimulatory receptor CD28 is a primary target for PD-1-mediated inhibition. *Science* 2017; **355**:1428–1433.

42 Kamphorst AO, Wieland A, Nasti T, Yang S, Zhang R, Barber DL, *et al.* Rescue of exhausted CD8 T cells by PD-1-targeted therapies is CD28-dependent. *Science* 2017; **355**:1423–1427.

43 Ny L, Jespersen H, Karlsson J, Alsén S, Filges S, All-Eriksson C, *et al.* The PEMDAC phase 2 study of pembrolizumab and entinostat in patients with metastatic uveal melanoma. *Nat Commun* 2021; **12**:5155.

44 Castle JC, Kreiter S, Diekmann J, Löwer M, van de Roemer N, de Graaf J, *et al.* Exploiting the mutanome for tumor vaccination. *Cancer Res* 2012; **72**:1081–1091.

45 Bhadury J, Nilsson LM, Muralidharan SV, Green LC, Li Z, Gesner EM, *et al.* BET and HDAC inhibitors induce similar genes and biological effects and synergize to kill in Myc-induced murine lymphoma. *Proc Natl Acad Sci U S A* 2014; **111**:E2721–E2730.

46 Jespersen H, Lindberg MF, Donia M, Söderberg EMV, Andersen R, Keller U, *et al.* Clinical responses to adoptive T-cell transfer can be modeled in an autologous immune-humanized mouse model. *Nat Commun* 2017; **8**:707.

47 Huang D, Rossini E, Steiner S, Caflisch A. Structured water molecules in the binding site of bromodomains can be displaced by cosolvent. *ChemMedChem* 2014; **9**:573–579.

48 Remke N, Bisht S, Oberbeck S, Nolting J, Brossart P. Selective BET-bromodomain inhibition by JQ1 suppresses dendritic cell maturation and antigen-specific T-cell responses. *Cancer Immunol Immunother* 2021; **70**:107–121.

49 Schilderink R, Bell M, Reginato E, Patten C, Rioja I, Hilbers FW, *et al.* BET bromodomain inhibition reduces maturation and enhances tolerogenic properties of human and mouse dendritic cells. *Mol Immunol* 2016; **79**:66–76.

50 Toniolo PA, Liu S, Yeh JE, Moraes-Vieira PM, Walker SR, Vafaizadeh V, *et al.* Inhibiting STAT5 by the BET bromodomain inhibitor JQ1 disrupts human dendritic cell maturation. *J Immunol* 2015; **194**:3180–3190.

51 Chee J, Wilson C, Buzzai A, Wylie B, Forbes CA, Booth M, *et al.* Impaired T cell proliferation by ex vivo BET-inhibition impedes adoptive immunotherapy in a murine melanoma model. *Epigenetics* 2020; **15**:134–144.

52 Gibbons HR, Mi DJ, Farley VM, Esmond T, Kaood MB, Aune TM. Bromodomain inhibitor JQ1 reversibly blocks IFN-γ production. *Sci Rep* 2019; **9**:10280.

53 Veneziani I, Fruci D, Compagnone M, Pistoia V, Rossi P, Cifaldi L. The BET-bromodomain inhibitor JQ1 renders neuroblastoma cells more resistant to NK cell-mediated recognition and killing by downregulating ligands for NKG2D and DNAM-1 receptors. *Oncotarget* 2019; **10**:2151–2160.

54 Jespersen H, Olofsson Bagge R, Ullenhag G, Carneiro A, Helgadottir H, Ljuslinder I, *et al.* Concomitant use of pembrolizumab and entinostat in adult patients with metastatic uveal melanoma (PEMDAC study): protocol for a multicenter phase II open label study. *BMC Cancer* 2019; **19**:415.

55 Figueiredo CR, Kalirai H, Sacco JJ, Azevedo RA, Duckworth A, Slupsky JR, *et al.* Loss of BAP1 expression is associated with an immunosuppressive microenvironment in uveal melanoma, with implications for immunotherapy development. *J Pathol* 2020; **250**:420–439.